Editors' Suggestion

Coherent control of photomagnetic back-switching by double-pump laser pulses

T. Zalewski[ORCID],[*] L. Nowak[ORCID], and A. Stupakiewicz[ORCID]
Faculty of Physics, University of Bialystok, 1L Ciolkowskiego, 15-245 Bialystok, Poland

The control of nonthermal all-optical magnetization switching, under a regime of a train of identical laser pulses, opens up opportunities for ultrafast magnetic recording. Here, we investigate the photomagnetic back-switching capabilities of the write and erase magnetic domain pattern using double-pump pulse excitations in an iron-garnet film with pure cubic magnetocrystalline symmetry. It is essential to note that forward and backward magnetization switching is achievable in two distinctive scenarios: using identical linearly polarized laser pulses and with pulses having orthogonal polarization planes. By observing the switch of magnetization at domains independent of the initial state, one can nonthermally toggle the magnetization, equivalent to the XOR logic operation, at frequencies reaching up to 50 GHz.

DOI: 10.1103/PhysRevApplied.21.044026

I. INTRODUCTION

In the past decade, several mechanisms finally leading to the ultrafast all-optical switching (AOS) of magnetization in both metals and dielectric materials have been shown [1]. Qualitatively, magnetization switching solely using a laser pulse can be either nondeterministic—every incident pulse can switch the magnetization, resulting in toggle switching—or deterministic—the polarized laser pulse introduces some kind of break in the symmetry, which determines the switching between two states of magnetization. In the case of thermal-based ultrafast AOS in metallic materials [2,3], both regimes of magnetization switching have already been demonstrated [4–6]. For instance, for deterministic switching, the degeneracy between magnetic states can be broken by the helicity of circularly polarized light. In such all-optical helicity-dependent switching (AO-HDS) [2,6–8], the final state of magnetization is controlled and determined by the left or right circular polarization of the optical pulse. On the other hand, in specific materials, such as Gd-based alloys, multisublattice alloys such as Gd/Co [9], or synthetic multilayers with nanostructures of Gd/Co [10] and Tb/Co [11,12], the magnetization can only be switched by a single femtosecond pulse, regardless of its polarization state. This all-optical helicity-independent switching [3,10,11] gives a toggle effect, making the final magnetization state dependent on the parity of incident pulses.

In the case of dielectric materials, ultrafast magnetization control can be achieved through thermal effects [13]. However, when based on the photomagnetic effect, it does not entail heat loading, making switching a nonthermal

process. It has been experimentally shown that in yttrium iron garnet doped with cobalt (YIG:Co) [14], it is possible to permanently switch the magnetization state within only 20 ps by using a single ultrashort linearly polarized laser pulse. Light-pulse polarization along the [100] or [010] axis resonantly excites a specific d-d transition in Co ions, modifying the magnetic anisotropy. This photoinduced anisotropy can lift the degeneracy between domain states, thus permanently switching the magnetization. This has been demonstrated in YIG:Co films with a 4° miscut angle, showing that using the femtosecond laser pulse can write, erase, and rewrite magnetic domains only after changing the orientation of linear polarization at frequencies up to 20 GHz [15].

The determination of possible frequencies and repetition times for controlling the magnetization state can be directly obtained by employing double-pump pulses separated by a defined time delay. This method was recently commonly applied in the case of metallic ferrimagnets, such as Gd-Fe-Co [16,17] or Tb-Fe-Co [18], where the recovery time after thermally induced changes was crucial. Reducing this recovery time accelerates writing and erasing cycles [19,20]. This approach is also relevant for the half-metallic Heusler ferrimagnet $Mn_2Ru_{0.9}Ga$ [21], as well as in the case of AO-HDS in Pt/Co/Pt [22]. Furthermore, a subsequent optical pulse provides an additional degree of freedom in controlling magnetization dynamics through different mechanisms, such as the coherent control of spin waves in ferrimagnetic garnets [23] or the magnetoacoustic mechanism driven by quasistatic strain [24].

Recently, the nonthermal-toggle switching regime observed in YIG:Co films with pure magnetocrystalline cubic symmetry [25] was shown. Here, for distinction from

_____
[*]Corresponding author: tmkzlwsk@uwb.edu.pl

the thermal-based toggle switching, we refer to this regime as the back-switching of magnetization. In this regime, the magnetization state can be controlled solely by the sequence of femtosecond laser pulses without changing their polarization direction. Control of the back-switching regime with the precessional mechanism of magnetization switching raises several questions. First, if one pulse can switch magnetization and a subsequent pulse can reverse it, what will happen if both of these pulses appear together? On the other hand, from an application perspective, where the change in the direction of magnetization from "down" to "up" corresponds to the bit state "1," and the reverse corresponds to "0," the lack of necessity to control the laser polarization state for writing and erasing magnetic "bits" can significantly simplify the device. This eliminates the need for changing the laser polarization at high frequencies to match the recording speed. Although thermal-based all-optical switching in metallic materials has been successfully integrated into the form of a magnetic tunnel junction, in which switching is read out by measuring the tunneling magnetoresistance, paving the way towards a different category of optospintronics devices [26,27], the search for alternative materials and ways to develop beyond-CMOS technology remains an open question. While integrating dielectric materials into spintronics presents an ongoing challenge, photomagnetic switching offers obvious advantages due to its nonthermal character.

II. EXPERIMENTAL DETAILS

We used YIG:Co thin films with the composition $Y_2CaFe_{3.9}Co_{0.1}GeO_{12}$ and a thickness of 8 μm. The garnet film was grown using the liquid-phase epitaxy method on the (001) plane of the gadolinium gallium garnet ($Gd_3Ga_5O_{12}$) substrate with a miscut of <0.1°. The dominant negative cubic magnetic anisotropy, $K_c = -5.5 \times 10^3$ erg/cm^3, with a small uniaxial contribution aligned along the [001] crystal-growth direction with constant $K_u = 0.6 \times 10^3$ erg/cm^3 results in four energetically equivalent easy-magnetization axes along the cube diagonals of the $\langle 111 \rangle$-type directions [Fig. 1(b)]. The pure cubic magnetocrystalline-symmetry-domain structure observed in magneto-optical microscopy is balanced, with magnetic domains covering equivalent volumes and forming a uniformly distributed labyrinth pattern. The garnet is characterized by a Curie temperature of $T_C = 455$ K, saturation magnetization of $4\pi M_s = 75$ G, and Gilbert damping of $\alpha = 0.19$.

To observe the magnetic domain pattern and magnetization switching, we utilized a magneto-optical microscope in Faraday geometry, as presented in Fig. 1(a). The magnetization dynamics of photomagnetic switching were examined using the time-resolved pump and probe technique [28] utilizing a double-pump excitation scheme [15,17].
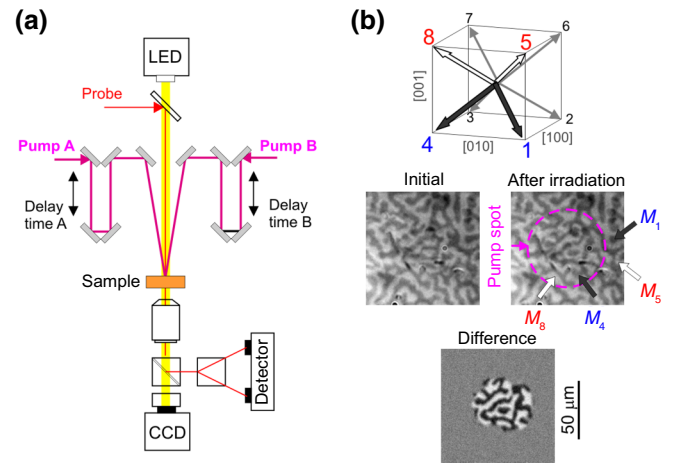

FIG. 1. (a) Scheme of the double-pump and probe experimental setup in Faraday geometry used for measuring magnetization precession and imaging of the domain structure and its switching. Both pumps A and B use their own delay lines, allowing for a precise definition of the time delay (A or B) between a single-pump beam and a probe beam, Δt, or between two pump pulses, Δt_{AB}. (b) Magnetic domain structure with easy-magnetization-axis orientation in YIG:Co films and magneto-optical images presenting the initial domain structure and the switched structure after irradiation by a single-pump pulse. By applying an 80-Oe external magnetic field with a time duration of about 1 s along the [1−10] or [110] directions, the initial domain structure containing specific pairs of magnetic states (M_1/M_5 and M_8/M_4) can be selected. After the magnetic field is removed, the magnetic pattern stays stable. Due to the labyrinthlike and difficult-to-distinguish character of the changes in the domain structure, all subsequent images are presented in a difference form created by subtracting images before and after irradiation. Marked magnetization states correspond to states aligned along $M_1 \parallel$ [11−1], $M_4 \parallel$ [1−1−1], $M_5 \parallel$ [11−1], and $M_8 \parallel$ [1−11] directions.

As a source of laser pulses, the setup utilized an ultrafast Ti:sapphire laser system that provided a train of pulses with a duration of 35 fs, wavelength of 800 nm, and base repetition rate of 1 kHz. The beam was split into three separate branches. One of them, maintaining the central 800-nm wavelength, was used as a probe beam. Two pumps, referred to as pump A and pump B, were directed to separate optical parametric amplifiers, enabling wavelength conversion and selecting the 1300-nm wavelength. Next, the beams were directed toward separate mechanical delay lines, which allowed for adjusting the mutual delay between the first pump, A, and the second pump, B, set as the Δt_{AB} time. The probe beam illuminated the sample at normal incidence and two pump beams were directed at an angle of about ±10° from normal incidence. All measurements were performed without an external magnetic field and at room temperature.

Since back-switching can be observed in the statics regime, in which the exposure time enabling

magneto-optical images to be obtained can be arbitrarily long and last several hundred milliseconds, in a relatively simple experiment using double-pump excitation, we were able to analyze pump-pulse pair interference. First, we precisely adjusted the optical parameters of pumps A and B to match each other. The pump fluence (50 mJ/cm^2), polarization plane along the [100] crystallographic orientation in the YIG:Co film, and the localization on the sample were unified to provide the exact switching area using a single laser pulse of either A or B. The laser pump-fluence range was adjusted to match that of a previously investigated YIG:Co film [14]. The optical absorption in our garnet films at 1300 nm was about 12%. The estimated energy of local laser-induced heat loading for the fluence used, 50 mJ/cm^2, is about 8 J/cm^3, which increases the temperature of garnet by only 4 K. This value is significantly smaller than the heat loading in any kind of heat-induced toggle switching.

In the absence of an external magnetic field, the observed domain structure, as presented in Fig. 1(b) appears as labyrinthlike domains covering equivalent volumes. The tracing of the out-of-plane magnetization component ([001] magnetization direction) distinguishes two magnetization states. In the case of our garnet films with the (001) plane, magnetization in the "1" and "4" states (or "8" and "5" states) has equal normal projections, and thus, at normal light incidence the contrast in these domains looks identical, see Fig. 1(b). To verify the presence of all four different domain phases, the sample can be tilted approximately 15° from the (001) plane with a simultaneously applied in-plane magnetic field of about 20 Oe along the [110] or [1−10] directions [29], allowing for the simultaneous visualization of out-of-plane and in-plane magnetization components in the magneto-optical Faraday geometry. When exposing the structure to a pump pulse, capable of inducing switching and back-switching, only the out-of-plane component is visualized, disregarding the in-plane component, and thus, the specific magnetic state, regardless of the initial state or magnetic history. Achieving a toggle regime of switching within a single pulse under these conditions introduces full nondeterministicity, as the selection of the initial state does not influence the switching, as represented here by a local change in the out-of-plane component.

III. DOUBLE-PUMP BACK-SWITCHING

Next, the sample was excited by both pulses A and B, which were in spatiotemporal overlap. By delaying pulse B and increasing Δt_{AB}, a full set of double-pump images was captured. Notably, precise adjustments were made to beam focusing, positioning, and fluences of A and B, ensuring an exact match. This resulted in the same switching pattern being achievable with a single A or B beam pulse, as illustrated in Fig. 2(a) (single-pump image), showcasing

switching between the [11−1] and [1−11] magnetization directions. Differentiation was achieved by subtracting the initial image of the sample from the image obtained after exposing the sample to a pump pulse. Importantly, without specific temporal synchronization, subsequent pulses from either beam A or B, regardless of the polarization direction (parallel to the [100] or [010] axis), provide back-switching [25].

To quantitatively analyze the impact of the second pump pulse on switching, we expressed the efficiency of double-pump switching as a normalized switching area to the area switched by a single-pump pulse. For every image, the normalized switching area was determined as an area encompassing the entire switched spot, translating the switching size into switching efficiency. During double-pump excitation, magnetization switching occurs up to $\Delta t_{AB} = 320$ ps. The dependence of the switching area for Δt_{AB} time is depicted in Fig. 2(b). This obtained time-dependent trace is characterized by three zones. To understand this shape, measurements involving double-pump time-resolved measurements with pulse fluences of 10 mJ/cm^3 are required.

To conduct these measurements, we utilized a double-pump and probe setup capable of time-resolved tracking of magnetization precession for pump laser fluence (<10 mJ/cm^2) below the switching threshold. In this configuration, the probe beam, operating at a 1-kHz repetition rate and focused on the sample with a diameter of 50 μm polarized orthogonally to the pump-pulse polarization was employed. To detect temporal changes in the Faraday rotation signal, which is proportional to the magnetization component (M_z) along the [001] crystallographic direction in the sample, a scheme with an autobalanced photodiode was used. After traversing the sample, the probe beam was directed to a half-wave plate and a Wollaston prism, which separated it into two linearly polarized beams with orthogonal polarization. These beams were directed to two separate branches of an autobalanced photodiode, which monitored the change in their intensities corresponding to Faraday rotation. In this case, for every particular delay between pulses A and B, the probe beam was swept with the delay Δt, revealing the impact of both pump beams on magnetization precession. Both pump pulses were once again equalized and matched to individually induce exactly the same precession signal.

The obtained time-resolved double-pump traces are presented in Fig. 2(c), with arrows marking the position of pump pulse B. We note that for $\Delta t_{AB} = 0$ ps, the mutual overlap of the laser pulses causes constructive interference, enhancing the effective amplitude of precession. Therefore, the overlapping of two identical laser pulses increased the amplitude of photomagnetic precession and switching area [see Fig. 2(b)] by a factor of 2. The precession amplitude was determined using an exponentially damped sine function to fit the data. The superposition of the pump
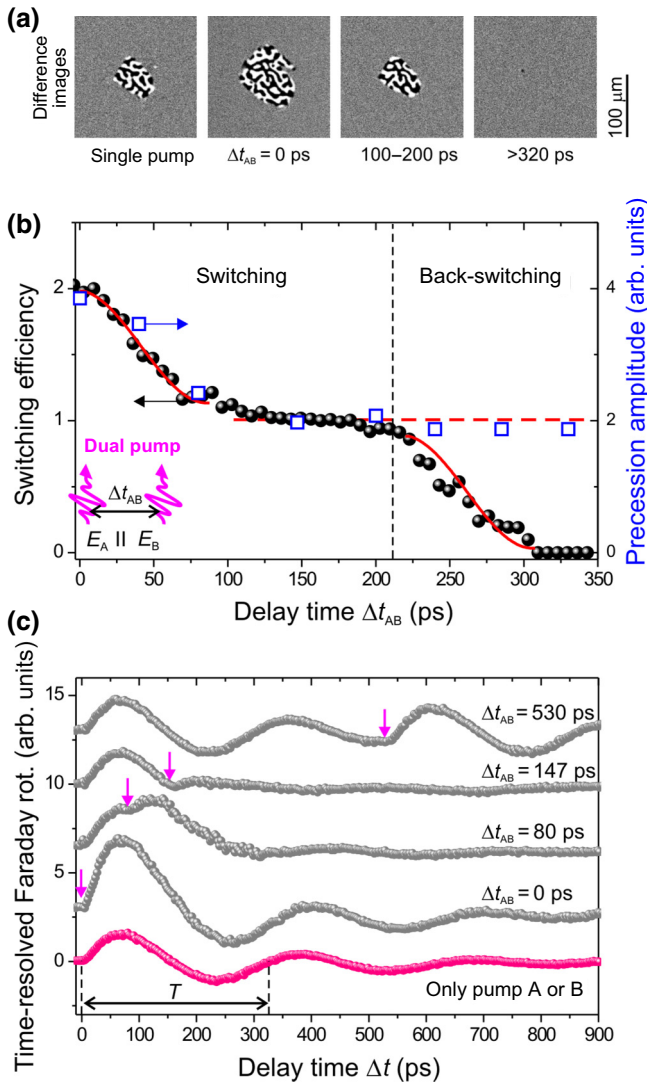
FIG. 2. (a) Magneto-optical difference images presenting a double-pulse writing sequence with two identical pump pulses A and B with polarization E_A and E_B along the [100] axes and delayed by Δt_{AB}. First image shows switching after excitation with either a single A or B pump pulse. Subsequent images present the obtained switching pattern during double-pump pulse excitation with the marked delay, Δt_{AB}. (b) Normalized switched area as a function of delay time, Δt_{AB} (circled black points). Solid red line directing to the saturation regions was fitted using $\cos(2\pi\Delta t_{AB}/t_{sw})$, where $t_{sw} = (178.6 \pm 5.2)$ ps is the half period of magnetization precession (T) [14]. Square blue points represent the amplitude determined from the double-pump traces as the amplitude of magnetization precession. Dashed red line is a guide for the eye. (c) Time-resolved Faraday rotation signal from the only single-pump pulse (red points) and the double-pump and probe pulses for different times Δt_{AB}. Both pump pulses were polarized along the same polarization plane along the [100] direction in YIG:Co. Curves are offset vertically. Arrows mark the temporal position of pump pulse B, which is delayed by Δt_{AB}.

laser pulses effectively increases the amplitude, reaching its maximal value at $\Delta t_{AB} = 0$ and decreasing to the level

obtained by a single pulse in approximately $\Delta t_{AB} = 75$ ps. This correlates with the region of decreased switching efficiency. Furthermore, the two signals of magnetization precession start interfering with each other in counterphases, resulting in the freezing of magnetization precession after half the period T for $\Delta t_{AB} \sim 147$ ps [see Fig. 2(c)]. In this range, the effective amplitude is defined solely by pulse A, and the switching efficiency does not change up to about $\Delta t_{AB} = 210$ ps [see Fig. 2(b)], demonstrating the AND logic operation. Finally, for $\Delta t_{AB} > 210$ ps, the laser pulses are separated far enough that they cannot constructively interfere with subsequent sinelike precession to overcome the switching threshold, as a single effective pulse. Therefore, in the switching regime for pump laser pulses with a fluence of 50 mJ/cm^3, while the first pulse, A, provides switching, the second, B, starting from a position with already almost stopped magnetization motion, provides a separate stimulus resulting in back-switching. Such a regime is equivalent to the XOR logic operation. Complete back-switching occurs at $\Delta t_{AB} > 320$ ps, which can be correlated with the magnetization-precession period of frequency. In contrast, as observed in the same composition of the YIG:Co film with a miscut, the switching state after the second pulse remained stable above 200 ps. Such an observation further confirms the precession-amplitude dependence [dashed line in Fig. 2(b)], suggesting that, after this time, the effect of a sequence of pulses remains constant, and the subsequent state will be the same as the initial one. It is worth noting that pulse fluence significantly influences both the switching efficiency and dynamic measurements. For instance, as demonstrated in Ref. [15], mutual interference of two pump fluences below the switching threshold can surpass the threshold and provide switching. Moreover, very high fluences could potentially allow for interference between further oscillation maxima, resulting in more "steps" in the switching-area dependence in Fig. 2(c).

To demonstrate the repeatability of photomagnetic switching within a single-pump pulse on the picosecond timescale, we captured a series of single-shot time-resolved images using the pump and probe setup described in detail in Ref. [28]. The wavelengths and polarizations of laser pulses were identical to those specified for pump and probe dynamics. However, the probe beam was defocused to a diameter larger than 500 μm to illuminate a sufficiently large area for imaging. The time-resolved magneto-optical image, generated by the rotation of the plane of polarization induced by the pump pulse, was captured on a synchronized CCD camera.

The exemplary stack of time-resolved pump and probe differential images is presented in Fig. 3(a), with the temporal evolution of the magnetic contrast, proportional to the normalized out-of-plane magnetization component, ΔM_z, shown in Fig. 3(b). Two characteristic image pairs (1,2 and 3,4) of subsequent pump pulses shot at the

beginning of the switching process [images 1,2 with the delay time (A or B) as a difference between pump and probe, $\Delta t_1 = 40$ ps] and after the switching process (images 3,4 and $\Delta t_2 = 147$ ps) are shown. In this experiment, we did not apply an external resetting magnetic field, as was done previously in the YIG:Co sample with a miscut, allowing for the observation of back-switching dynamics driven by subsequent single-pump pulses in time-resolved images. Unexpectedly, we achieved magnetization reversal from the [11−1] to [1−11] direction and vice versa without resetting. This confirms the previously observed toggle-switching regime [25], in which the end state of switching becomes the initial state for the subsequent pulse. It is evident that the contrast develops rapidly for 20−90 ps. Comparing this timescale to the precession signal, shown in Fig. 2(c) with a precession period of $T = 320$ ps, in good agreement with the frequency of the ferromagnetic resonance mode [30,31], it can be seen that switching can occur within about the quarter-precession-period timescale. However, as in the case of samples with a miscut angle, the switching trajectory within different domains is characterized by asymmetry in two types of trajectories: towards $M+$ and $M-$ magnetization states along the [1−11] and [11−1] directions, respectively [see Fig. 3(b)] [32].

To demonstrate a resetting scenario, we utilize two pump pulses polarized orthogonally to each other. Using the same approach and settings, we performed analogous measurements, only changing the polarization plane of pump pulse B. The obtained measurements are provided in the same manner, with the exemplar stack of differential images of the domain pattern being presented in Fig. 4(a), the normalized switching-area dependence utilizing double-pump excitation being presented in Fig. 4(b), and the double-pump and probe time-resolved magnetization dynamics being presented in Fig 4(c).

With pump A polarized along the [100] axis and pump B polarized along the [010] axis, the generated torque has opposite signs. Therefore, for $\Delta t_{AB} = 0$ ps, precessional signals in counterphases interfere destructively, resulting in no magnetization precession, and therefore, do not provide any switching. In contrast to previous results for the YIG:Co miscut sample, this confirms the existence of pure cubic symmetry and energetic equivalence of direction of magnetization during forward and backward switching. However, by increasing Δt_{AB}, a characteristic region between $\Delta t_{AB} = 30$ and 80 ps, in which switching is obtainable, occurs. Once again, to understand this behavior, insight into dynamics is required. As observed, when precession traces are delayed, the interference changes its character and starts to provide precession similar to that obtained by a single pump. A further increase of Δt_{AB} increases the amplitude of precession to the saturated level; however, after about a quarter of the precession period, $T/4$, the second pump pulse, B, is able to overcome
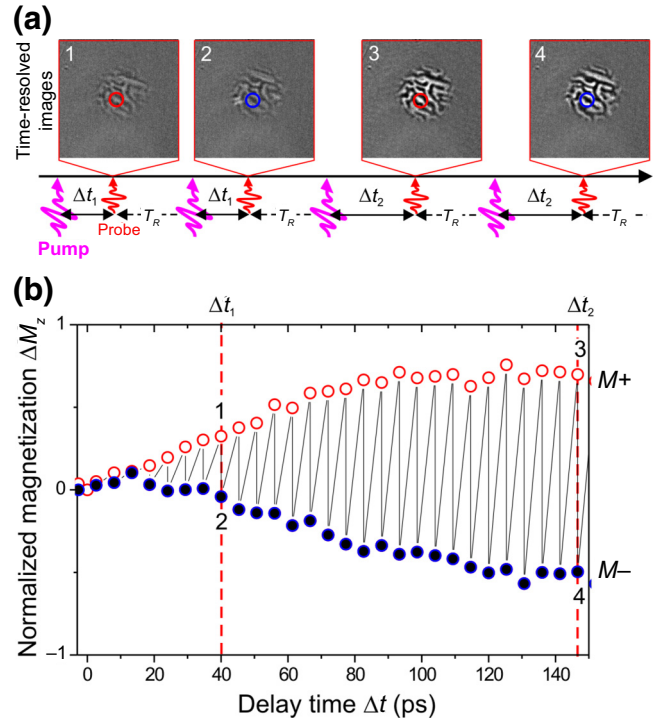

FIG. 3. (a) Differential single-shot time-resolved images of the magnetic pattern obtained at $\Delta t_1 = 40$ ps and $\Delta t_2 = 147$ ps. Each subsequent image starts as an initial state for the next pump-pulse switching. Observed change in the image intensity corresponds to the change in the normalized magnetization component. Between every captured time-resolved image, the $T_R < 50$ ms time required for data acquisition; therefore, the initial state is always fully switched. (b) Time-resolved change of the Faraday rotation proportional to the change in the out-of-plane magnetization component, ΔM_z. Traces were retrieved from the image stack from the region marked by colored squares separately for both black, with $M-$ along the [11−1] direction, and white, $M+$ along the [1−11] direction, domains.

switching. It results once again in switching with pulse A and magnetization reversal with pulse B.

IV. CONCLUSIONS

These results underline that the photomagnetic back-switching regime, with the precessional motion of magnetization, opens a plethora of possibilities for writing and erasing magnetic bits using only a sequence of ultrashort laser pulses. In this regime, the lifetime of photoinduced anisotropy is limited to approximately 20 ps and is independent of the initial state of magnetization with a fixed laser-polarization state. We note that the energetically equivalent magnetization states in our garnet provide symmetry of writing and erasing during the switching and back-switching processes. Thus, together with the lack of necessity to change the polarization state of pump pulses, it does not require additional energy to be invested, just
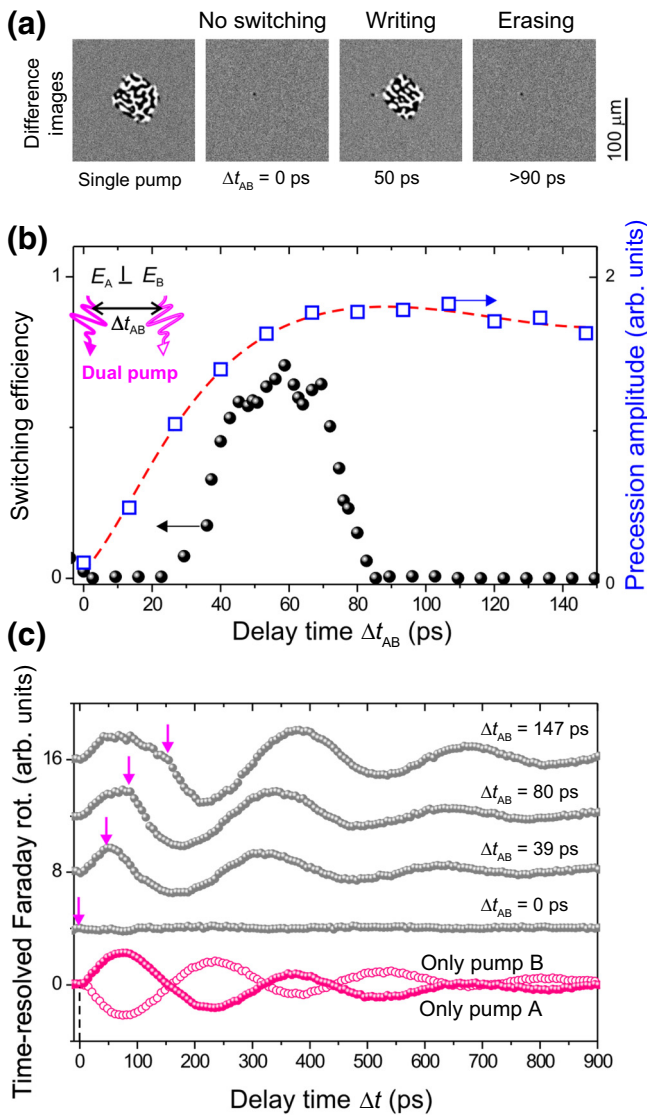
FIG. 4. (a) Magneto-optical difference images presenting a double-pulse writing sequence with two pulses A with E_A || [100] axis and B with E_B || [010] axis. As previously, the first image shows switching after excitation with either a single A or B pump pulse with the size used for normalization. Subsequent image represents the obtained switched pattern depending on Δt_{AB}. (b) Normalized switched area as a function of delay time, Δt_{AB} (circled black points). Square blue points represent the amplitude determined from the double-pump traces as the amplitude of magnetization precession. Dashed line represents the effective precession amplitude of both pump pulses. (c) Time-resolved Faraday-rotation signal from the double-pump and probe setup with pump A polarized along the [100] plane and pump B along the [010] plane. Notably, the two pump signals, being in counterphase, interfere completely destructively, $\Delta t_{AB} = 0$ ps.

control of the repetition rate and intensity of the laser pulses. Therefore, the magnetization state can be toggled for laser pulses with control of the delay time between pulses, achieving a switching frequency of up to 50 GHz.

The toggle switching regime can also be successfully used to perform basic logic operations, such as XOR, AND, or inverting operations equivalent to NOT. In fact, the utilization of only a set of AND and NOT connectives provides functional completeness, giving access to any other logic operation, as every switching function can be expressed by means of operations within it. It is crucial to emphasize that all discussed operations are driven by coherent control of precession, signifying no involvement of quantum operations. Supporting and controlling magnetization switching, for example, both laser and electric pulses, could provide an additional degree of freedom in the modification of an extrinsic contribution to magnetic anisotropy in the photomagnetic garnets. This potential advancement could find utility in emerging fields, such as optospintronics or optomagnonics, utilizing the multistate character of the garnet and metallic systems.

Data that support the findings of this study are available from the corresponding author upon reasonable request.

[1] A. V. Kimel, A. M. Kalashnikova, A. Pogrebna, and A. K. Zvezdin, Fundamentals and perspectives of ultrafast photoferroic recording, Phys. Rep. **852**, 1 (2020).

[2] C. D. Stanciu, F. Hansteen, A. V. Kimel, A. Kirilyuk, A. Tsukamoto, A. Itoh, and T. Rasing, All-optical magnetic recording with circularly polarized light, Phys. Rev. Lett. **99**, 047601 (2007).

[3] T. A. Ostler, *et al.*, Ultrafast heating as a sufficient stimulus for magnetization reversal in a ferrimagnet, Nat. Commun. **3**, 666 (2012).

[4] M. S. El Hadri, P. Pirro, C. H. Lambert, S. Petit-Watelot, Y. Quessab, M. Hehn, F. Montaigne, G. Malinowski, and S. Mangin, Two Types of all-optical magnetization switching mechanisms using femtosecond laser pulses, Phys. Rev. B **94**, 064412 (2016).

[5] C. S. Davies, J. H. Mentink, A. V. Kimel, T. Rasing, and A. Kirilyuk, Helicity-independent all-optical switching of magnetization in ferrimagnetic alloys, J. Magn. Magn. Mater. **563**, 169851 (2022).

[6] Jung-Wei Liao, Pierre Vallobra, Liam O'Brien, Unai Atxitia, Victor Raposo, Dorothée Petit, Tarun Vemulkar, Gregory Malinowski, Michel Hehn, Eduardo Martínez, Stéphane Mangin, and Russell P. Cowburn, Controlling all-optical helicity-dependent switching in engineered rare-earth free synthetic ferrimagnets, Adv. Sci. **6**, 1901876 (2019).

[7] S. Mangin, M. Gottwald, C. H. Lambert, D. Steil, V. Uhlíř, L. Pang, M. Hehn, S. Alebrand, M. Cinchetti, G. Malinowski, Y. Fainman, M. Aeschlimann, and E. E. Fullerton, Engineered materials for all-optical helicity-dependent magnetic switching, Nat. Mater. **13**, 286 (2014).

[8] R. Medapalli, D. Afanasiev, D. K. Kim, Y. Quessab, S. Manna, S. A. Montoya, A. Kirilyuk, T. Rasing, A. V. Kimel, and E. E. Fullerton, Multiscale dynamics of helicity-dependent all-optical magnetization reversal in ferromagnetic Co/Pt multilayers, Phys. Rev. B **96**, 224421 (2017).

[9] A. El-Ghazaly, B. Tran, A. Ceballos, C. H. Lambert, A. Pattabi, S. Salahuddin, F. Hellman, and J. Bokor, Ultrafast magnetization switching in nanoscale magnetic dots, Appl. Phys. Lett. **114**, 232407 (2019).

[10] M. L. M. Lalieu, M. J. G. Peeters, S. R. R. Haenen, R. Lavrijsen, and B. Koopmans, Deterministic all-optical switching of synthetic ferrimagnets using single femtosecond laser pulses, Phys. Rev. B **96**, 220411(R) (2017).

[11] L. Avilés-Félix, A. Olivier, G. Li, C. S. Davies, L. Álvaro-Gómez, M. Rubio-Roy, S. Auffret, A. Kirilyuk, A. V. Kimel, Th. Rasing, L. D. Buda-Prejbeanu, R. C. Sousa, B. Dieny, and I. L. Prejbeanu, Single-shot all-optical switching of magnetization in Tb/Co multilayer-based electrodes, Sci. Rep. **10**, 5211 (2020).

[12] K. Mishra, T. G. H. Blank, C. S. Davies, L. Avilés-Félix, D. Salomoni, L. D. Buda-Prejbeanu, R. C. Sousa, I. L. Prejbeanu, B. Koopmans, Th. Rasing, A. V. Kimel, and A. Kirilyuk, Dynamics of all-optical single-shot switching of magnetization in Tb/Co multilayers, Phys. Rev. Res. **5**, 023163 (2023).

[13] M. Deb, P. Molho, B. Barbara, and J. Y. Bigot, Controlling laser-induced magnetization reversal dynamics in a rare-earth iron garnet across the magnetization compensation point, Phys. Rev. B **97**, 134419 (2018).

[14] A. Stupakiewicz, K. Szerenos, D. Afanasiev, A. Kirilyuk, and A. V. Kimel, Ultrafast nonthermal photo-magnetic recording in a transparent medium, Nature **542**, 71 (2017).

[15] K. Szerenos, A. V. Kimel, A. Maziewski, A. Kirilyuk, and A. Stupakiewicz, Fundamental limits on the repetition rate of photomagnetic recording, Phys. Rev. Appl. **12**, 044057 (2019).

[16] U. Atxitia and T. A. Ostler, Ultrafast double magnetization switching in GdFeCo with two picosecond-delayed femtosecond pump pulses, Appl. Phys. Lett. **113**, 062402 (2018).

[17] Sicong Wang, Chen Wei, Yuanhua Feng, Hongkun Cao, Wenzhe Li, Yaoyu Cao, Bai-Ou Guan, Arata Tsukamoto, Andrei Kirilyuk, Alexey V. Kimel, and Xiangping Li, Dual-shot dynamics and ultimate frequency of all-optical magnetic recording on GdFeCo, Light: Sci. Appl. **10**, 2047 (2021).

[18] T. Cheng, J. Wu, T. Liu, X. Zou, J. Cai, R. W. Chantrell, and Y. Xu, Dual-pump manipulation of ultrafast demagnetization in TbFeCo, Phys. Rev. B **93**, 064401 (2016).

[19] F. Steinbach, N. Stetzuhn, D. Engel, U. Atxitia, C. Von Korff Schmising, and S. Eisebitt, Accelerating double pulse all-optical write/erase cycles in metallic ferrimagnets, Appl. Phys. Lett. **120**, 112406 (2022).

[20] D. Liu, C. Jiang, N. Wang, and C. Xu, Minimum separation between two pump pulses for ultrafast double magnetization switching in GdFeCo, Appl. Phys. Lett. **123**, 162401 (2023).

[21] C. Banerjee, K. Rode, G. Atcheson, S. Lenne, P. Stamenov, J. M. D. Coey, and J. Besbas, Ultrafast double pulse all-optical reswitching of a ferrimagnet, Phys. Rev. Lett. **126**, 177202 (2021).

[22] K. T. Yamada, A. V. Kimel, K. H. Prabhakara, S. Ruta, T. Li, F. Ando, S. Semin, T. Ono, A. Kirilyuk, and T. Rasing, Efficient all-optical helicity dependent switching of spins in a Pt/Co/Pt film by a dual-pulse excitation, Front. Nanotechnol. **4**, 765848 (2022).

[23] M. Deb, E. Popova, H. Y. Jaffrès, N. Keller, and M. Bargheer, Controlling high-frequency spin-wave dynamics using double-pulse laser excitation, Phys. Rev. Appl. **18**, 044001 (2022).

[24] M. Mattern, F.-C. Weber, D. Engel, C. Korff-Schmising, and M. Bargheer, Coherent control of magnetization precession by double-pulse activation of effective fields from magnetoacoustics and demagnetization, ArXiv Phys. 2311.04803 (2023).

[25] T. Zalewski, A. Maziewski, A. V Kimel, and A. Stupakiewicz, Ultrafast all-optical toggle writing of Magnetic bits without relying on heat, ArXiv Phys. 2311.10173 (2023).

[26] J.-Y. Chen, L. He, J.-P. Wang, and M. Li, All-optical switching of magnetic tunnel junctions with single subpicosecond laser pulses, Phys. Rev. Appl. **7**, 021001 (2017).

[27] A. V. Kimel and M. Li, Writing magnetic memory with ultrashort light pulses, Nat. Rev. Mater. **4**, 189 (2019).

[28] T. Zalewski and A. Stupakiewicz, Single-shot imaging of ultrafast all-optical magnetization dynamics with a spatiotemporal resolution, Rev. Sci. Instrum. **92**, 103004 (2021).

[29] A. Maziewski, Unexpected magnetization processes in YIG + Co films, J. Magn. Magn. Mater. **88**, 325 (1990).

[30] A. Stupakiewicz, M. Pashkevich, A. Maziewski, A. Stognij, and N. Novitskii, Spin precession modulation in a magnetic bilayer, Appl. Phys. Lett. **101**, 262406 (2012).

[31] A. Frej, I. Razdolski, A. Maziewski, and A. Stupakiewicz, Nonlinear subswitching regime of magnetization dynamics in photomagnetic garnets, Phys. Rev. B **107**, 134405 (2023).

[32] T. Zalewski, V. A. Ozerov, A. Maziewski, I. Razdolski, and A. Stupakiewicz, Nonreciprocal coherent all-optical switching between magnetic multistates, Phys. Rev. B **109**, L060303 (2024).